netochemical data. The TIP term is somewhat large; we suspect it is an artifact due to the presence of impurities and is, therefore, not very important.

The interdimer coupling obtained from the above analysis (−11.2 cm^{-1}) is typical of the weak antiferromagnetic interactions observed for Fe(III) dimers containing hydroxo or alkoxo bridging.[3,4,15] Although the Fe–OR–Fe bridging angle for the interdimer bridges is large, the extent of superexchange coupling for $^6A_{1g}$ Fe(III) generally appears to be quite insensitive toward variations in bridging angles.[3,4] The intradimer coupling (−63.4 cm^{-1}) is well below the values (−90 to −120 cm^{-1})[3,12] usually observed for oxo-bridged Fe(III) dimers. Owing to the weak antiferromagnetic coupling that carboxylate-bridged Fe(III) systems are thought to exhibit,[3] coupling via the carbonate probably is negligible relative to that via the oxo-bridge. The closest approximation to the "dimer" subunit of the tetranuclear complex **1** is the oxo-bridged Fe(III) binuclear complex with additional phosphodiester bridging that recently has been characterized by Armstrong and Lippard.[23] This latter binuclear complex exhibits typical antiferromagnetic superexchange ($J = -98$ cm^{-1}). The Fe–O(oxo) distances [1.812 (5), 1.804 (5) Å] and Fe–O(oxo)–Fe angle [134.7 (3)°] are close to those observed for the corresponding structural features of **1**. However, additional coordination to the Fe–O–Fe unit can change the coupling constant significantly. Thus, coordination of a third Fe(III) to an Fe_2O core at a distance of 2.067 Å causes the Fe–O(oxo) bond distances to increase (1.862 (7), 1.867 (7) Å) and coupling within the Fe_2O unit to decrease to −55 cm^{-1}.[24] These bond distances and the superexchange coupling are intermediate between those reported for typical oxo-bridged Fe(III) binuclear complexes and oxo-bridged Fe(III) trinuclear complexes [Fe–O = 1.92–1.96 Å, $J \approx -30$ cm^{-1}].[3] The reason for the unexpectedly low intradimer coupling in **1** may be that the Fe–O(oxo) bond distances have elongated just to the point where the superexchange coupling becomes significantly attenuated. The factors responsible for the slight elongation of the Fe–O(oxo) bond distances in **1** cannot be identified with certainty. Possibly, this effect is due to strain within the tetranuclear cluster or to subtle electronic effects associated with the carbonato bridging. Packing of the tetranuclear complex precludes the approach of lattice water to the O(13) and O(13′) atoms, while structural parameters of the Fe_2O(oxo) unit rule out hydroxo-bridging and thus the presence of two protons situated about the center of the cluster between O(13) and O(13′). As noted above, however, we cannot rule out the presence of a single H^+ at (ordered) or near (disordered structure) the center of the cluster. The presence of this H^+ ion would serve to lengthen the Fe–O(oxo) bonds and reduce the extent of antiferromagnetic coupling. The reduced antiferromagnetism ($J \approx -77$ cm^{-1}) reported for oxyhemerythrin presumably is related to the clear H-bonding interaction observed between the hydroperoxide ligand and the oxo-bridge.[10b]

Acknowledgment. Research at Rutgers University was supported by a crystallographic instrumentation grant from the National Institutes of Health (Grant 1510 RRO 1486 01A1), and research at the University of Illinois was supported by National Institutes of Health Grant HL13652.

Registry No. $Na_6(\mathbf{1})\cdot\approx 20H_2O$, 105597-77-1.

Supplementary Material Available: Listing of anisotropic thermal parameters, H atom parameters, and magnetic susceptibility data (3 pages); observed and calculated structure factor tables (16 pages). Ordering information is given on any current masthead page.

Hydride Transfer in the Oxidation of Alcohols by $[(bpy)_2(py)Ru(O)]^{2+}$. A k_H/k_D Kinetic Isotope Effect of 50

Lee Roecker and Thomas J. Meyer*

Contribution from the Department of Chemistry, The University of North Carolina, Chapel Hill, North Carolina 27514. *Received June 2, 1986*

Abstract: The kinetics of oxidation of a series of alcohols by $[(bpy_2(py)Ru^{IV}(O)]^{2+}$ (bpy is 2,2′-bipyridine and py is pyridine) have been studied in aqueous solution and in acetonitrile. The reactions are first order in both alcohol and $Ru^{IV}{=}O^{2+}$, pH independent from pH 1.0 to 6.8, and slightly slower in acetonitrile than in water. Rate constants for oxidation increase with substituent as follows: methyl < primary < secondary < allylic ≲ benzylic. Tertiary alcohols are unreactive, and in the series of para substituted benzylic alcohols, $X–C_6H_4CH_2OH$ (X = CH_3O, CH_3, H, F, Cl, CF_3, and NO_2), the rate of oxidation is relatively insensitive to the substituent X. In aqueous solution k ranges from (3.5 ± 0.1) × 10^{-4} M^{-1} s^{-1} for the oxidation of methanol ($\Delta H^{\ddagger}$ = 14 ± 2 kcal/mol, $\Delta S^{\ddagger}$ = −26 ± 6 eu) to 2.43 ± 0.03 M^{-1} s^{-1} for the oxidation of benzyl alcohol ($\Delta H^{\ddagger}$ = 5.8 ± 0.4 kcal/mol, $\Delta S^{\ddagger}$ = −38 ± 1 eu). Large C–H kinetic isotope effects are observed, but solvent isotope effects are negligible. For CH_3OH compared to CD_3OH, k_H/k_D = 9 at 25 °C and for benzyl alcohol, $C_6H_5CH_2OH$ compared to $C_6H_5CD_2OH$, k_H/k_D = 50 ± 3 at 25 °C. Spectral evidence, in conjunction with the isotope effect data, suggests that oxidation of alcohols by $[(bpy)_2(py)Ru^{IV}(O)]^{2+}$ occurs by a two-electron, hydride transfer.

Oxidation of a variety of alcohols by oxo complexes of ruthenium have been reported over the past 20 years, but few mechanistic details are known.[1,2] Notable exceptions include the work of Lee and co-workers who have observed a primary kinetic isotope effect of 4.6 (25 °C, 1.94 M $HClO_4$) in the oxidation of 2-propanol to acetone by RuO_4^{2-} and who observe the formation of cyclobutanone from the oxidation of cyclobutanol by RuO_4 and RuO_4^{2-} suggestive of a two-electron, hydride transfer oxidation pathway.[3,4] An attractive feature associated with reagents like RuO_4 is that

(1) Lee, D. G.; van den Engh, M. In *Oxidation in Organic Chemistry, Part B*; Trahanovsky, W. S., E.; Academic Press: New York, 1973.
(2) Gagne, R. R.; Marks, D. N. *Inorg. Chem.* **1984**, *23*, 65 and references therein.
(3) Lee, D. G.; van den Engh, M. *Can. J. Chem.* **1972**, *50*, 2000.
(4) Lee, D. G.; Spitzer, U. A.; Cleland, J.; Olson, M. E. *Can. J. Chem.* **1976**, *54*, 2124.

0002-7863/87/1509-0746$01.50/0

they can be used catalytically in the presence of a suitable co-oxidant such as sodium periodate or hypochlorite,[5] but RuO_4 is a fairly unselective oxidant, and carbon–carbon bond cleavage is often a competitive process. Green et al. have met with some success at developing more selective reagents by using ligand modified complexes[6] such as $[Ru(bpy)(O)_2(Cl)_2]$ and $[Ru(O)_2(Cl)_3]^-$ where nearly quantitative conversion of a variety of alcohols to their corresponding aldehydes in nonaqueous solvents was observed.

Polypyridyl monooxo complexes of Ru(IV), e.g., $[(bpy)_2(py)Ru^{IV}(O)]^{2+}$ (bpy is 2,2′-bipyridine; py is pyridine), are particularly attractive as stoichiometric and catalytic oxidants, for several reasons:[7] (1) there is a versatility in the background synthetic chemistry which allows changes to be made in the ligands and consequently in the reduction potential while maintaining the oxidatively active $Ru^{IV}{=}O$ site. (2) The complexes have been used as electrocatalytic oxidants in aqeuous solution for a variety of substrates including alcohols. (3) Given the spectral and redox properties of the complexes and their inherent stability, it is relatively easy to obtain detailed kinetic, thermodynamic, and mechanistic information about their reactions. Previous mechanistic work has suggested, for example, that the oxidation of tertiary aromatic hydrocarbons proceeds via a "solvent assisted" hydride transfer[9]

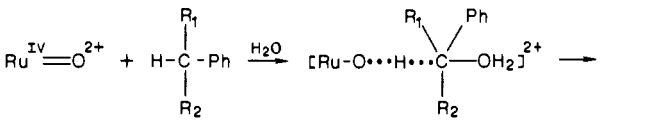

$$Ru^{II}\text{-}OH^{+} + PhR_1R_2COH_2^{+} \quad (1)$$

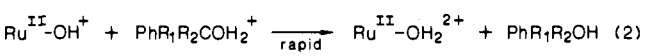

(2)

and the oxidation of 2-propanol to acetone by a hydride transfer pathway.[10]

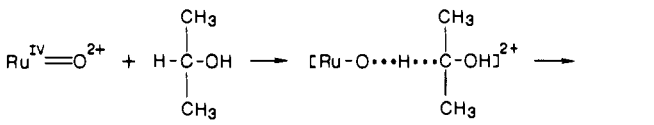

$$Ru^{II}\text{-}OH^{+} + (CH_3)_2COH^{+} \quad (3)$$

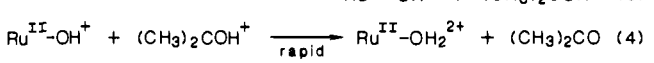

(4)

We report here the results of a rate and mechanistic study on the oxidation of a variety of alcohols by $[(bpy)_2(py)Ru(O)]^{2+}$. The goals of the work were first to attempt to define the hydride transfer pathway in further detail and, at the same time, to begin the process of assembling the experimental information required to deal with such complex pathways quantitatively, ultimately, at the level of understanding currently enjoyed by simple electron transfer.

Experimental Section

Materials. House-distilled water was redistilled from alkaline permanganate. Deuterium oxide, 99.8 atom % (Aldrich), acetone (Burdick and Jackson), acetonitrile (Burdick and Jackson), and doubly distilled perchloric acid (G. Frederick Smith) were used without additional purification. Acetonitrile (Baker) was distilled immediately before use from P_2O_5 under an argon atmosphere. Tetraethylammonium perchlorate (TEAP) was prepared by a literature procedure[11] and recrystallized 3 times from water. All other materials were reagent grade and were used without additional purification.

Preparations. The salts $[(bpy)_2(py)Ru(OH_2)](ClO_4)$, $[(bpy)_2(py)Ru(O)](ClO_4)$,[12] [(trpy)(phen)$Ru(OH_2)](ClO_4)$,[13] and [(trpy)(phen)$Ru(O)](ClO_4)_2$[13] were prepared by previously reported procedures.

Unless noted, all substrates were obtained from the Aldrich Chemical Co. and purified by vacuum distillation, recrystallization, sublimation, or silica gel chromatography. Purity was verified by TLC and/or ^1H NMR. Deuterated aromatic alcohols were prepared by reduction of the appropriate methyl or ethyl benzoate or ketone with $LiAlD_4$ in dry ethyl ether. A typical procedure is outlined below for the synthesis of dideuteriophenylcarbinol (benzyl alcohol-α,α-d_2).

$LiAlD_4$ (1.18 g, 28.1 mmol) was added to 100 mL of dry ethyl ether and cooled in an ice bath. Ethyl benzoate (5 mL, 35.0 mmol) in 50 mL of ethyl ether was slowly added. The solution was brought to room temperature and heated at reflux for 6 hours. The next day, 2 mL of 10% NaOH and 2 mL of H_2O were added; the resulting salts were filtered, and the filtrate was extracted with 2 × 50-mL portions of ethyl ether. The ether solutions were combined, dried over Na_2SO_4, and rotoevaporated to a clear oil. The crude product was purified by elution from silica gel, grade 923, 100–200 mesh (Aldrich) with 20% ethyl acetate/80% hexanes. The desired fractions were rotoevaporated to a clear oil (4 mL). TLC indicated only the presence of the alcohol. FT-NMR showed no residual solvent and complete deuteration at the benzylic positions.

CD_3OD, 99.5 atom % (Aldrich), was used without additional purification.

Instrumentation. UV–vis spectra were recorded on a Hewlett Packard 8450A diode array spectrophotometer. Stopped-flow measurements were carried out on an Amino–Morrow stopped-flow apparatus attached to a Beckman DU monochrometer. Conventional mixing experiments were performed on a Varian Series 634 spectrophotometer. Temperature was maintained to ±0.1 °C with a Brinkman Lauda RM6 temperature bath or a Forma Scientific Model 2095 temperature bath. Calculations were performed on a Commodore PET Computer Model 4032 by using locally written programs.

Kinetic Measurements in Water. Rate data for the disappearance of Ru(IV) were collected by following absorbance increases for the Ru(II) and Ru(III) products. The wavelengths used were 397 nm for $[(bpy)_2(py)Ru(O)]^{2+}$ and 400 nm for $[(trpy)(phen)Ru(O)]^{2+}$. These wavelengths are isosbestic points for the related $Ru^{III}\text{–}OH^{2+}$ and $Ru^{II}\text{–}OH_2^{2+}$ complexes, and, as such, the disappearance of Ru(IV) can be monitored without interference from the subsequent reduction of Ru(III) to Ru(II) which is considerably slower. Plots of $\ln|A_\infty - A_t|$ vs. time were linear for at least 4 half-lives, and first-order rate constants were calculated on the basis of a least-squares fit (uniform weighting) to the relation

$$\ln|A_\infty - A_t| = -kt + \ln|A_\infty - A_0|$$

where A_∞ is the final absorbance at completion of the reaction, A_0 is the initial absorbance, A_t is the absorbance measured at time t, and k is the first-order rate constant. A_∞ readings were obtained for each run, and data from the first 3 half-lives were used in determining k.

Reactant solutions containing aromatic alcohols and 3-buten-2-ol were usually prepared in 1:1 acetone/0.20 M $HClO_4$. The remaining alchol solutions were prepared in 0.10 M phosphate buffer (pH 6.8) or 0.20 or 0.0024 M $HClO_4$ (μ = 0.16 M, $NaClO_4$). Kinetic runs were initiated by mixing an equivalent volume of an aqueous Ru(IV) solution with the alcohol solution. Substrate concentrations were calculated from the known densities of the liquid alcohols or for the case of solid substrates by dissolving a known amount of alcohol in the solvent and diluting to a known volume.

Purging reactant solutions with argon prior to use had no apparent effect on the kinetics, so no attempts were made to deoxygenate the solutions.

Kinetic Measurements in Acetonitrile. In acetonitrile complications arise from the fact that the reduced Ru(II) product $[(bpy)_2(py)Ru^{II}(OH_2)]^{2+}$ undergoes solvolysis ($t_{1/2}$ = 8 min at 23 °C) to yield the acetonitrile complex,[10] and $[(bpy)_2(py)Ru^{III}(OH)]^{2+}$ reacts slowly ($k \sim 10^{-5}$ M^{-1} s^{-1}) with acetonitrile to give an uncharacterized product.[10] Both complications can be circumvented if the alcohol oxidations are sufficiently rapid. Since the initial ruthenium product is $Ru^{II}(OH_2)^{2+}$ or $Ru^{III}(OH)^{2+}$, rapid reactions could be monitored at 397 nm, and an

(5) (a) Carlson, P. H. J.; Katsuki, T.; Martin, V. S.; Sharpless, K. B. *J. Org. Chem.* **1981**, *46*, 3936. (b) Schuda, P. F.; Cichowiz, M. B.; Heimann, M. R. *Tetrahedron Lett.* **1983**, *24*, 3829. (c) Charkraborti, A. K.; Ghatak, U. R. *Synthesis* **1983**, 746. (d) Burke, L. D.; Healy, J. F. *J. Chem. Soc. Dalton Trans.* **1982**, 1091.

(6) Green, G.; Griffith, W. P.; Hollinshead, D. M.; Lee, S. V.; Schroder, M. *J. Chem. Soc. Perkin Trans. 1* **1984**, 681.

(7) (a) Meyer, T. J. *J. Electrochem. Soc.* **1984**, *131*, 221C. (b) Roecker, L. Ph.D. Dissertation, The University of North Carolina, 1985.

(8) (a) Thompson, M. S.; De Giovani, W. F.; Moyer, B. A.; Meyer, T. J. *J. Org. Chem.* **1984**, *49*, 4972. (b) Meyer, B. A.; Thompson, M. S.; Meyer, T. J. *J. Am. Chem. Soc.* **1980**, *102*, 2310.

(9) Thompson, M. S.; Meyer, T. J. *J. Am. Chem. Soc.* **1982**, *104*, 5070.

(10) Thompson, M. S.; Meyer, T. J. *J. Am. Chem. Soc.* **1982**, *104*, 4106.

(11) Sawyer, D. T.; Roberts, J. L., Jr. *Experimental Electrochemistry for Chemists*; Wiley: New York, 1974; p 212.

(12) Moyer, B. A.; Meyer, T. J. *Inorg. Chem.* **1981**, *20*, 436.

(13) Roecker, L.; Kutner, W.; Gilbert, J. A.; Simmons, M.; Murray, R. W.; Meyer, T. J. *Inorg. Chem.* **1985**, *24*, 3784.

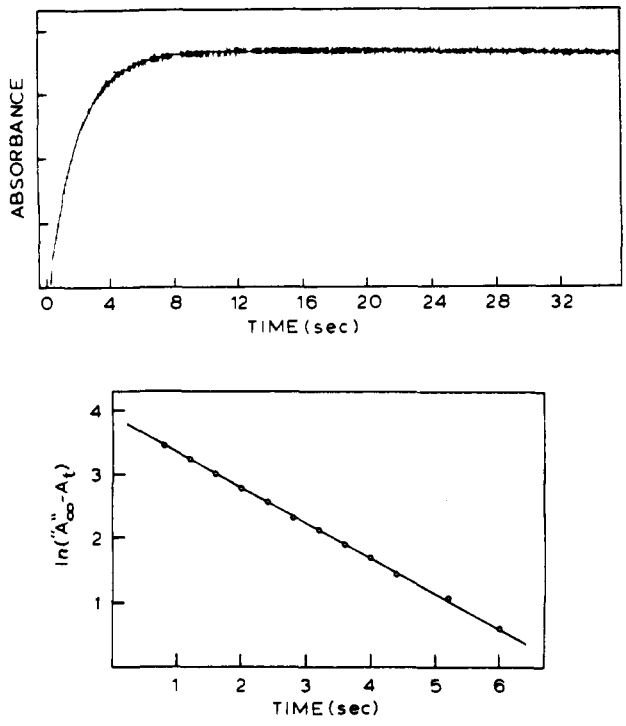

Figure 1. Absorbance trace and ln $|"A_\infty" - A_t|$ vs. time plot for the oxidation of benzyl alcohol by $[(bpy)_2(py)Ru(O)]^{2+}$ in 0.10 M TEAP/CH_3CN at 397 nm. For the definition of "A_∞" see text.

artifical "A_∞" reading obtained before interference by acetonitrile solvolysis. This artifical "A_∞" reading would be obtained if the reaction was complete in 40 s or less. As illustrated in Figure 1, plots of ln $|"A_\infty" - A_t|$ vs. time were linear. In slower runs, data from the first 40 s were used in a Guggenheim analysis[14] to obtain values of k. At some substrate concentrations, both methods of data analysis were used, and values obtained by the two methods agree to within 2%.

For the oxidation of benzyl alcohol in acetonitrile, plots of k_{obsd} vs. substrate concentration were nonlinear[7b] but became linear in the presence of 0.10 M TEAP, and the rate constants reported in Table I were obtained in solutions that were 0.10 M in TEAP. Identical results were obtained by using acetonitrile that had not been distilled from P_2O_5 before use.

For the oxidation of 4-nitrobenzyl alcohol plots of ln $|A_\infty - A_t|$ vs. time were nonlinear in both acetonitrile and acetone/water, and k was estimated from data taken during the first 2 half-lives.

All data collected are available as supplementary material.

Product Analysis and Stoichiometry. Product analyses and stoichiometries for several of the substrates examined here have been reported previously. In the case of 2-propanol, the product was found to be acetone quantitatively.[10] Under electrocatalytic conditions primary alcohols are oxidized to mixtures of the corresponding aldehyde and acid.[8] To avoid possible kinetic complications introduced by subsequent aldehyde oxidation, the alcohol concentrations were kept in large excess in the kinetic runs.

Results

Spectral Changes. Shown in Figure 2 are the spectral changes that accompany the oxidation of benzyl alcohol by $[(bpy)_2(py)Ru(O)]^{2+}$ in aqueous acid. Two stages are evident. In the initial stages of the reaction (lower traces) an isosbestic point appeared at 343 nm along with a peak at 312 nm. In the later stages of the reaction (upper traces) the isosbestic point at 343 nm disappeared and was replaced by isosbestic points at 322, 370, and 397 nm; the peak at 312 nm decreased while a peak at 470 nm appeared. The isosbestic points match those which appear in the electrochemical reduction of $[(bpy)_2(py)Ru^{IV}(O)]^{2+}$ to $[(bpy)_2(py)Ru^{III}(OH)]^{2+}$ and of $[(bpy)_2(py)Ru^{III}(OH)]^{2+}$ to $[(bpy)_2(py)Ru^{II}(OH_2)]^{2+}$ in water.[12] Thus the faster, initial spectral changes can be attributed to oxidation by $[(bpy)_2(py)Ru^{IV}(O)]^{2+}$ and the slower spectral changes to oxidation by $[(bpy)_2(py)Ru^{III}(OH)]^{2+}$. By monitoring the reaction at 397 nm, an isosbestic point between Ru(III) and Ru(II), the oxidation by Ru(IV) could be investigated without interference from the subsequent oxidation by Ru(III).

(14) Espenson, J. H. *Chemical Kinetics and Reaction Mechanisms*; McGraw Hill: New York, 1981; p 25.

Table I. Second-Order Rate Constants for the Oxidation of Alcohols by $[(bpy)_2(py)Ru(O)]^{2+}$ at 25 °C

substrate	medium[a]	k (M^{-1} s^{-1})
methanol	0.012 M $HClO_4$, μ = 0.08 M ($NaClO_4$)	$(3.5 \pm 0.1) \times 10^{-4}$
	pH 6.8, μ = 0.10 M, phosphate buffer	3.5×10^{-4}
ethanol	0.012 M $HClO_4$, μ = 0.08 M ($NaClO_4$)	$(2.1 \pm 0.1) \times 10^{-3}$
1-propanol	0.012 M $HClO_4$, μ = 0.08 M ($NaClO_4$)	$(6.2 \pm 0.1) \times 10^{-3}$
2-propanol	pH 6.8, μ = 0.32 M[b] (Li_2SO_4)	$(6.7 \pm 0.1) \times 10^{-2}$
	CH_3CN[c]	$(8.7 \pm 0.9) \times 10^{-3}$
cyclohexanol[d]	pH 6.8, μ = 0.32 M (Li_2SO_4)	$(6.3 \pm 0.2) \times 10^{-2}$
2-propen-1-ol	0.10 M $HClO_4$	1.10 ± 0.02
	10% CH_3OH	1.07 ± 0.04
3-buten-2-ol	acetone/H_2O	1.09 ± 0.03
benzyl alcohol	0.10 M $HClO_4$	2.43 ± 0.03
	acetone/H_2O	2.42 ± 0.07
	10% CH_3OH	2.50 ± 0.09
	CH_3CN	1.54 ± 0.08
4-methoxybenzyl alcohol	acetone/H_2O	2.96 ± 0.05
4-nitrobenzyl alcohol	acetone/H_2O	3.0 ± 0.3
	CH_3CN	2.0 ± 0.3
4-fluorobenzyl alcohol	acetone/H_2O	1.92 ± 0.06
	CH_3CN	1.32 ± 0.03
4-fluorobenzyl alcohol[e]	acetone/H_2O	3.5×10^{-3}
4-methylbenzyl alcohol	CH_3CN	2.54 ± 0.08
sec-phenethyl alcohol	CH_3CN	2.63 ± 0.03
benzhydrol	acetone/H_2O[f]	3.00 ± 0.04
	CH_3CN	3.23 ± 0.05

[a] Acetone/H_2O refers to a 1/1/2 (by volume) solution of acetone/0.20 M $HClO_4/H_2O$; $[H^+]$ = 0.05 M, μ = 0.05 M. CH_3CN refers to 0.10 M TEAP/CH_3CN 10% CH_3OH refers to 10% by volume of CH_3OH added to water. [b] From ref 10, $[(trpy)(bpy)Ru(O)]^{2+}$ is the oxidant. [c] From ref 10, no TEAP. [d] From ref 8. [e] Rate of reaction with Ru(III), $[(bpy)_2(py)Ru(OH)]^{2+}$. [f] 60% acetone/40% 0.20 M $HClO_4$.

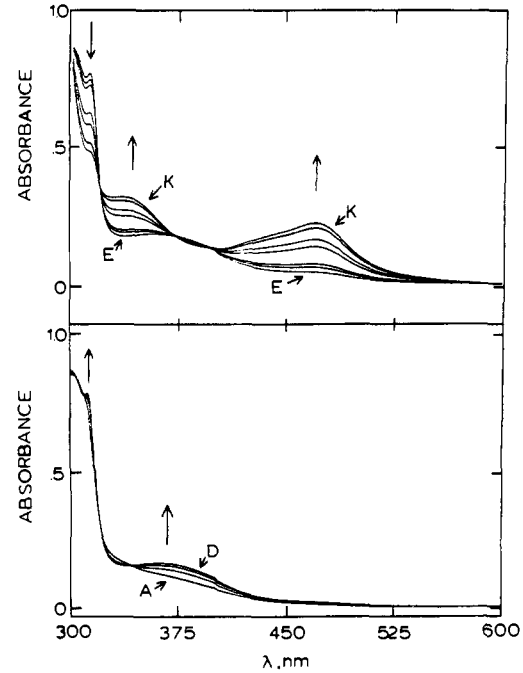

Figure 2. Successive spectral scans during the oxidation of benzyl alcohol by $[(bpy)_2(py)Ru(O)]^{2+}$ in 0.10 M $HClO_4$: (A) 5, (B) 10, (C) 15, (D) 20, (E) 50, (F) 75, (G) 100, (H) 360, (I) 660, (J) 1560, and (K) 2160 s after mixing.

Table II. Solvent and Substrate Kinetic Isotope Effects for the Oxidation of Alcohols by $[(bpy)_2(py)Ru(O)]^{2+}$ at 25 °C

substrate	medium[a]	k (M^{-1} s^{-1})	n[b]	k_{H_2O}/k_{D_2O}	k_H/k_D
methanol	H_2O	3.8×10^{-4}	1	1.1	
methanol	D_2O	3.5×10^{-4}	1		
methanol	pH 6.8, 0.10 M, phosphate buffer	3.8×10^{-4}	1		9
methanol-α,α,α-d_3	pH 6.8, 0.10 M, phosphate buffer	4.4×10^{-5}	1		
ethanol	H_2O	4.5×10^{-3}	1	1.1	
ethanol	D_2O	4.3×10^{-3}	1		
benzyl alcohol	H_2O	2.32	1	1.0	
benzyl alcohol	D_2O	2.21	1		
benzyl alcohol	acetone/H_2O	2.42	12		50 ± 3
benzyl-α,α-d_2 alcohol	acetone/H_2O	0.049	4		
benzyl alcohol	0.10 M $HClO_4$	2.43	4		50
benzyl-α,α-d_2 alcohol	0.10 M $HClO_4$	0.048	2		
benzhydrol	acetone/H_2O	3.00	6		27 ± 3
benzhydrol-α-d	acetone/H_2O	0.11	3		
benzhydrol	CH_3CN	3.23	4		24 ± 2
benzhydrol-α-d	CH_3CN	0.14	3		
4-methylbenzyl alcohol	CH_3CN	2.54	4		50
4-methylbenzyl-α,α-d_2 alcohol	CH_3CN	0.05	1		
4-methoxybenzyl alcohol	acetone/H_2O	3.0	2		50
4-methoxybenzyl-α,α-d_2 alcohol	acetone/H_2O	0.06	1		

[a] Solvent compositions as in Table I. [b] n is the number of independent determinations used to calculate k.

Kinetics. Under the conditions studied the experimental rate law can be described by

$$-d[Ru(IV)]/dt = k[Alc][Ru(IV)] = k_{obsd}[Ru(IV)] \quad (5)$$

In aqueous solution or in 0.10 M TEAP/CH_3CN, k_{obsd} is linearly dependent on the alcohol concentration. Values of the second-order rate constants derived from such plots are given in Table I. The values were calculated by a linear least-squares procedure over at least a tenfold span of substrate concentration or, in instances where less data were collected, by dividing k_{obsd} by [Alc]. When checked, values of k derived from individual runs were generally within 3% of the values of k obtained in the least-squares procedure.

As observed for 2-propanol, rate constants for oxidation by $[(bpy)_2(py)Ru(O)]^{2+}$ exhibit no O_2 dependence and are independent of ionic strength in aqueous solution.[10] However, in the absence of added electrolyte some rate retardation can occur at high substrate concentrations, and it is notable that in CH_3CN without added electrolyte, plots of k_{obsd} vs. [Alc] were nonlinear with benzyl alcohol as substrate.[7b] A reasonable assumption to explain this behavior is that a preassociation occurs between reactants (K_A), and at high substrate concentrations, the con-

$$A + B \overset{K_A}{\rightleftharpoons} A,B \xrightarrow{k_2} D \quad (6)$$

centration of the association complex becomes appreciable. However, the appearance of the apparent preassociation was not pursued further, and subsequent experiments in CH_3CN were performed in 0.10 M TEAP where plots of k_{obsd} vs. [Alc] were linear over the range investigated.

Solvent Effects. To aid dissolution of water insoluble substrates some reactions were performed in methanol/water or acetone/water mixtures or in CH_3CN. Data in Table I show that with benzyl alcohol and 2-propen-1-ol the second-order rate constant is the same within experimental error in water as in the solvent mixtures but decreases slightly in CH_3CN.

Isotope Effects. Results are given in Table II for solvent and substrate kinetic isotope effects. Solvent isotope effects (k_{H_2O}/k_{D_2O}) for the oxidations of methanol, ethanol, and benzyl alcohol by $[(bpy)_2(py)Ru(O)]^{2+}$ are insignificant.

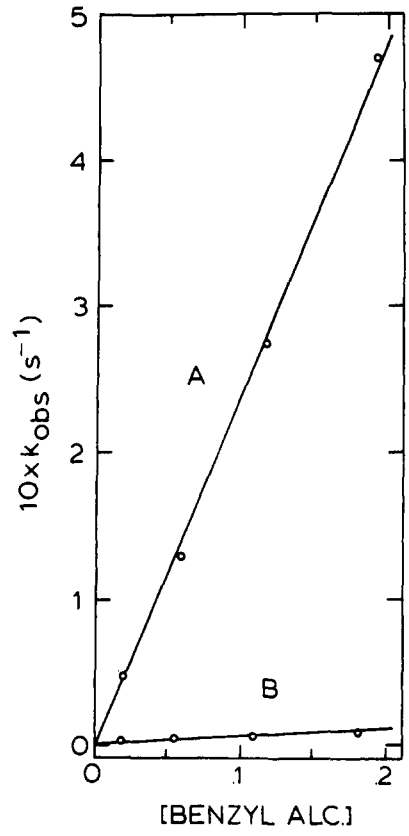

Figure 3. Plots of k_{obsd} vs. (A) $[C_6H_5CH_2OH]$ and (B) $[C_6H_5CD_2OH]$ at 25.0 ± 0.1 in acetone/water [1/1], μ = 0.05 M ($HClO_4$) for oxidation by $[(bpy)_2(py)Ru(O)]^{2+}$.

Large C–H deuterium isotope effects are observed in all cases where the effect was investigated. At 25 °C: for methanol, k_H/k_D = 9 (pH 6.8); for benzyl alcohol, k_H/k_D = 50 ± 3 (acetone/water); for benzhydrol, k_H/k_D = 27 ± 3 (acetone/water) and 24 ± 2 (CH_3CN); for 4-methoxybenzyl alcohol, k_H/k_D = 50 (acetone/water); and for 4-methylbenzyl alcohol, k_H/k_D = 50 (CH_3CN).

In Figure 3 are shown data for oxidation of benzyl alcohol and its deuteriated analogue in acetone/water. The result was reproduced in 0.10 M $HClO_4$ with an independently prepared sample of the deuteriated compound (see Supplementary Material Table B). The reported isotope effects for the 4-methoxy and 4-methylbenzyl alcohols are only estimates. Data analyzed by the Guggenheim method for the deuteriated compounds had poor correlation coefficients, and data for only a single substrate concentration were analyzed. The problem in obtaining reliable kinetic data with these substrates probably arises from the subsequent rapid oxidation of the initial aldehyde product.[15] Due to the slowness of the methanol oxidation, only a single concentration of CD_3OH was used.

To see if solvent contributed to the large isotope effects, the oxidation of benzhydrol was examined in 60% acetone/40% water and in CH_3CN (0.10 M TEAP). Within experimental error the primary kinetic isotope effect is the same in both media.

Activation Parameters. In Table III are listed activation parameters for the oxidation of various alcohols by $[(bpy)_2(py)Ru(O)]^{2+}$ obtained from plots of ln (k/T) vs. $1/T$. The plots are linear over the temperature ranges studied in each case. The entropy of activation, $\Delta S^{\ddagger}$, remains constant at −40 ± 2 eu for the primary, secondary, allylic, and benzylic alcohols independent of solvent, water vs. acetonitrile, with methanol being a distinct case. Enthalpies of activation, $\Delta H^{\ddagger}$, are slightly lower for the more reactive allylic and benzylic alcohols. For benzyl alcohol the k_H/k_D

(15) Preliminary experiments on the oxidation of aldehydes by $[(bpy)_2(py)Ru(O)]^{2+}$ show that for 1-propanal, k = 0.67 M^{-1} s^{-1} (0.012 M $HClO_4$, μ = 0.08 M, $NaClO_4$); benzaldehyde, k = 3.3 M^{-1} s^{-1} (CH_3CN); and for 4-methyl and 4-methoxybenzaldehyde, $k > 10^3$ M^{-1} s^{-1} (CH_3CN). Roecker, L.; Adrian, S., unpublished results.

Table III. Activation Parameters for the Oxidation of Alcohols by $[(bpy)_2(py)Ru(O)]^{2+}$

substrate	medium	$\Delta H^{\ddagger}$ (kcal/mol)	$\Delta S^{\ddagger}$ (eu)
2-propanol[a]	pH 6.8, μ = 0.32 M (Li_2SO_4)	9 ± 1	−34 ± 4
2-propanol[b]	CH_3CN	8 ± 1	−42 ± 5
methanol	pH 6.8, 0.10 M, phosphate buffer	14 ± 2	−26 ± 6
methanol-α,α,α-d_3	pH 6.8, 0.10 M, phosphate buffer	17 ± 2	−21 ± 5
ethanol	0.012 M $HClO_4$, μ = 0.08 M ($NaClO_4$)	9.0 ± 0.7	−40 ± 2
2-propen-1-ol	0.012 M $HClO_4$, μ = 0.08 M ($NaClO_4$)	6.9 ± 0.7	−38 ± 2
benzyl alcohol	CH_3CN/0.10 M TEAP	5.8 ± 0.4	−38 ± 1
benzyl alcohol	0.10 M $HClO_4$	5.7 ± 0.2	−38 ± 1
benzyl-α,α-d_2 alcohol	0.10 M $HClO_4$	5.6 ± 0.6	−46 ± 2

[a] From ref 10, $[(trpy)(bpy)Ru(O)]^{2+}$ is the oxidant. [b] From ref 10.

kinetic isotope effect lies entirely in the temperature independent terms: for $C_6H_5CH_2OH$ $\Delta S^{\ddagger} = -38 \pm 2$ eu compared to $\Delta S^{\ddagger} = -46 \pm 2$ eu for benzyl alcohol-α,α-d_2. For methanol the effect appears in both the temperature dependent and temperature independent terms: for CH_3OH $\Delta H^{\ddagger} = 14 \pm 2$ kcal/mol and $\Delta S^{\ddagger} = -26 \pm 6$ eu while for methanol-α,α,α-d_3, $\Delta H^{\ddagger} = 17 \pm 2$ kcal/mol and $\Delta S^{\ddagger} = -21 \pm 5$ eu.

One- vs. Two-Electron Transfer. The magnitude of the k_H/k_D isotope effect clearly points to an important role for the C–H bond in the redox step. The question remains, however, as to whether the redox step involves 2 equiv and the direct production of Ru(II) and aldehyde or ketone (two-electron)

$$Ru^{IV}{=}O^{2+} + R_1R_2CHOH \rightarrow Ru^{II}{-}OH^{+} + R_1R_2COH^{+}$$

followed by rapid proton equilibration, or an initial 1-equiv step

$$Ru^{IV}{=}O^{2+} + R_1R_2CHOH \rightarrow Ru^{III}{-}OH^{2+} + R_1R_2C^{\bullet}OH$$

followed by oxidation of $R_1R_2C^{\bullet}OH$ by $Ru^{IV}{=}O^{2+}$, $Ru^{III}{-}OH^{2+}$, or O_2.

The spectral changes in Figure 2 are consistent with the mechanisms illustrated in Scheme I. The fundamental difference

Scheme I

Mechanism A (one-electron)

$$2Ru^{IV}{=}O^{2+} + R_1R_2CHOH \rightarrow 2Ru^{III}{-}OH^{2+} + R_1R_2C{=}O \quad k_{IV}$$

$$2Ru^{III}{-}OH^{2+} + R_1R_2CHOH \rightarrow 2Ru^{II}{-}OH_2^{2+} + R_1R_2C{=}O \quad k_{III}$$

$$2Ru^{IV}{=}O^{2+} + 2R_1R_2CHOH \rightarrow 2Ru^{II}{-}OH_2^{2+} + 2R_1R_2C{=}O \quad \text{net}$$

Mechanism B (two-electron)

$$Ru^{IV}{=}O^{2+} + R_1R_2CHOH \rightarrow Ru^{II}{-}OH_2^{2+} + R_1R_2C{=}O \quad k_{IV}$$

$$Ru^{IV}{=}O^{2+} + Ru^{II}{-}OH_2^{2+} \rightarrow 2Ru^{III}{-}OH^{2+} \quad k_{com}$$

$$2Ru^{III}{-}OH^{2+} + R_1R_2CHOH \rightarrow 2Ru^{II}{-}OH_2^{2+} + R_1R_2C{=}O \quad k_{III}$$

$$2Ru^{IV}{=}O^{2+} + 2R_1R_2CHOH \rightarrow 2Ru^{II}{-}OH_2^{2+} + 2R_1R_2C{=}O \quad \text{net}$$

between the two is that the initial redox step, k_{IV}, in mechanism A represents the rate of a net *one*-electron step to give Ru(III) while in mechanism B, k_{IV} represents the rate of a *two*-electron step to give Ru(II).

In principle, a distinction between the two mechanisms can be made by observing whether the initial product is Ru(II) or Ru(III) since their absorption spectra are significantly different. However, there is a complication since $Ru^{II}{-}OH_2^{2+}$, once formed, undergoes a rapid comproportionation in H_2O [k(25 °C, μ = 0.1 M) = 2 × 10^5 M^{-1} s^{-1}] with $Ru^{IV}{=}O^{2+}$ to give $2Ru^{III}{-}OH^{2+}$.[17] On the time scale illustrated in Figure 2, the two mechanisms are indistinguishable. Nonetheless, a distinction between the one- and two-electron pathways can still be made *if* the reaction is carried out at high initial concentrations of alcohol where

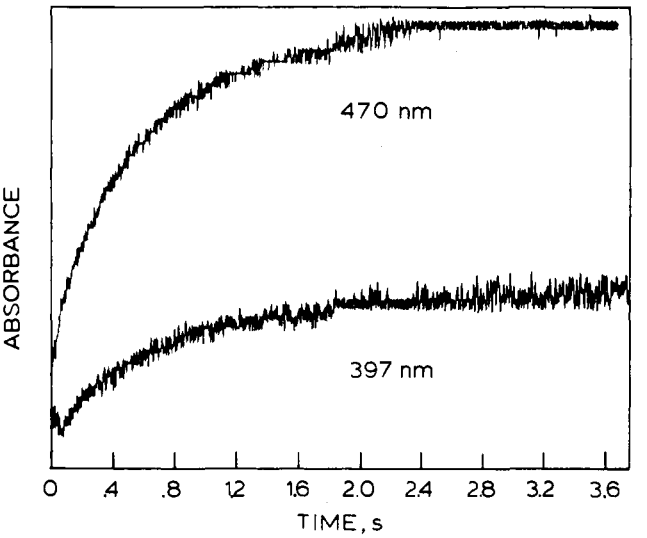

Figure 4. Absorbance traces obtained by stopped-flow monitoring of the oxidation of 2-propen-1-ol by $[(bpy)_2(py)Ru(O)]^{2+}$ in D_2O, [Alc] = 3.7 M, [Ru(IV)] = 1.63 × 10^{-5} M at 397 (lower trace) and 470 nm (upper trace).

$$k_{IV}[Alc][Ru(IV)] > k_{com}[Ru(IV)][Ru(II)] \quad (7)$$

by using stopped-flow monitoring. Rapid monitoring is required because of the following, slower oxidation of alcohol by $[(bpy)_2(py)Ru^{III}(OH)]^{2+}$ which gives $[(bpy)_2(py)Ru^{II}(OH)]^{2+}$ as the final Ru product. Application of this procedure to the oxidations of H_2O_2[19b] and HCO_2^-[20] has shown that $Ru^{III}{-}OH^{2+}$ is the initial product in the oxidation of H_2O_2 and $Ru^{II}{-}OH_2^{2+}$ in the oxidation of HCO_2^-.

With [benzyl alcohol] = 4.6 M in CH_3CN, the rate of disappearance of $Ru^{IV}{=}O^{2+}$ monitored at 397 nm in equal to the rate

(16) Wilkins, R. G. *The Study of Kinetics and Mechanism of Reactions of Transition Metal Complexes*; Allyn and Baoon; Boston, 1974.

(17) (a) Binstead, R. A.; Moyer, B. A.; Samuels, G. J.; Meyer, T. J. *J. Am. Chem. Soc.* **1981**, *103*, 2897. (b) Binstead, R. A.; Meyer, T. J. *J. Am. Chem. Soc.*, in press.

(18) Experimentally, we measure k_{com} = 4.5 × 10^4 with no added electrolyte in H_2O (μ = 0) which is a decrease of 4.4 compared to the value of 2 × 10^5 at μ = 0.1. The ratio of rates of comproportionation to oxidation for benzyl alcohol at μ = 0 is given by

$$\frac{rate_{com}}{rate_{ox}} = \frac{k_{com}[Ru(II)]}{k_{ox}[Alc]} = (1.9 \times 10^4)\frac{[Ru(II)]}{[Alc]}$$

where k_{ox} = 2.4 M^{-1} s^{-1} (Table I). At an initial concentration of [Ru(IV)] = 3.3 × 10^{-5} M with [Alc] = 4.5 M in water, even at the very end of the reaction where $[Ru(II)] \sim [Ru(IV)]_{init}$, the rate of comproportionation is less than 15% of the rate of oxidation. For the reactions in D_2O, k_{com} = 2.8 × 10^3 M^{-1} s^{-1} (μ = 0.0) and for oxidation of 2-propen-1-ol

$$\frac{rate_{com}}{rate_{ox}} = (4 \times 10^3)\frac{[Ru(II)]}{[Alc]}$$

At [Alc] = 3.7 M and $[Ru(IV)]_{init}$ = 1.6 × 10^{-5} M, the rate of comproportionation is less than 2% of the rate of oxidation at the end of the reaction. For 2-propanol

$$\frac{rate_{com}}{rate_{ox}} = (2.8 \times 10^5)\frac{[Ru(II)]}{[Alc]}$$

and at [Alc] = 9.1 M, $[Ru(IV)]_{init}$ = 5.4 × 10^{-6} M, the rate of comproportionation is less than 20% of the rate of oxidation at the end of the reaction.

(19) (a) Gilbert, J. A.; Gersten, S. W.; Meyer, T. J. *J. Am. Chem. Soc.* **1982**, *104*, 6872. (b) Gilbert, J. A.; Gersten, S. W.; Roecker, L.; Meyer, T. J. *Inorg. Chem.*, in press.

(20) Roecker, L.; Meyer, T. J. *J. Am. Chem. Soc.* **1986**, *108*, 4066.

of Ru^{II}–OH_2^{2+} appearance at 448 nm consistent with mechanism B and two-electron transfer.[18] In another experiment, a solid sample of $[(trpy)(phen)Ru(O)](ClO_4)_2$ was dissolved in neat benzyl alchol, and the resulting initial spectrum was that of Ru^{II}–OH_2^{2+}; no additional spectral changes were observed.

With substrates that were not as reactive as benzyl alcohol, similar experiments were performed in D_2O solutions since the rate of alcohol oxidation is unaffected by D_2O compared to H_2O, but the rate constant for comproportionation is decreased by a factor of 16 in D_2O.[17] For 2-propen-1-ol at 3.7 M, the rates of disappearance at 397 nm and appearance at 470 nm were identical (Figure 4) in D_2O solution.[18] With 2-propanol, a solid sample of $[(bpy)_2(py)Ru(O)](ClO_4)_2$ was added to a 9.14 M solution of 2-propanol in D_2O.[18] Absorbance traces after 50 s and after 15 min were identical and indicated that Ru(II) was the only ruthenium product in solution at all times.

The mixing experiments demonstrate that to an appreciable degree, Ru(II) must be the initial reduced form of the complex. If a series of one-electron steps were operative (Mechanism A in Scheme I), Ru(II) would have been only a minor component in the initial stages of the reactions given the relative rates of alcohol oxidation by Ru(IV) and Ru(III) (k_{IV}/k_{III} = 500 for the oxidations of 4-fluorobenzyl alcohol, see Table I, and k_{IV}/k_{III} = 1200 for the oxidation of 2-propanol.[10])

Discussion

Mechanistic Considerations. In addition to the rate law, a number of additional results bear directly on the question of mechanism. Most striking is the observation of large α C–H kinetic isotope effects for oxidations by $[(bpy)_2(py)Ru(O)]^{2+}$. Large C–H or O–H based kinetic isotope effects have also been reported for the reactions between $[(bpy)_2(py)Ru(O)]^{2+}$ and 2-propanol,[10] hydrogen peroxide,[19] formate,[20] hydroquinone,[21] and $[(bpy)_2(py)Ru^{II}(OH)_2)]^{2+}$.[17]

From the combination of rate law, kinetic isotope effect, and product studies, it seems that the dominant pathway for the oxidation of alcohols by polypyridyl monooxo complexes of Ru(IV) is two-electron in character and involves the carbon–hydrogen bond in an intimate way. The mechanism can be divided for convenience into an initial preassociation step between the reactants most probably followed by a redox step best described as "hydride transfer"

$$(bpy)_2(py)Ru^{IV}{=}O^{2+} + HC(OH)R_1R_2 \overset{K_a'}{\rightleftharpoons} (bpy)_2(py)Ru^{IV}{=}O^{2+}, HC(OH)R_1R_2 \quad (8)$$

$$(bpy)_2(py)Ru^{IV}{=}O^{2+}, HC(OH)R_1R_2 \xrightarrow{k_{redox}} [(bpy)_2(py)Ru{-}O\cdots H\cdots C(OH)R_1R_2]^{2+} \rightarrow (bpy)_2(py)Ru^{II}{-}OH^{+}, R_1R_2COH^{+} \quad (9)$$

followed by separation and rapid proton equilibration

$$(bpy)_2(py)Ru^{II}{-}OH^{+}, R_1R_2COH^{+} \rightarrow (bpy)_2(py)Ru^{II}{-}OH_2^{2+} + R_1R_2CO$$

With this interpretation the experimentally measured rate constant is, in fact, the product of the association constant, K_a', and the rate constant for the redox step, k_{redox}. Given the necessity for an intimate interaction between the $Ru{=}O^{2+}$ and $R_1R_2CH(OH)$ groups, K_a' is not simply the statistically derived association constant as calculated by the Eigen–Fuoss equation

$$K_a = \frac{4\pi N_o(r_A + r_B)^3}{3000}\exp(-w/RT) \quad (10)$$

which assumes spherical reactants of radii r_A and r_B and w is the electrostatic free-energy change arising from formation of the association complex.[22] Rather, K_a' is the product of a K_a-like term and an orientation factor reflecting the fraction of association

Scheme II

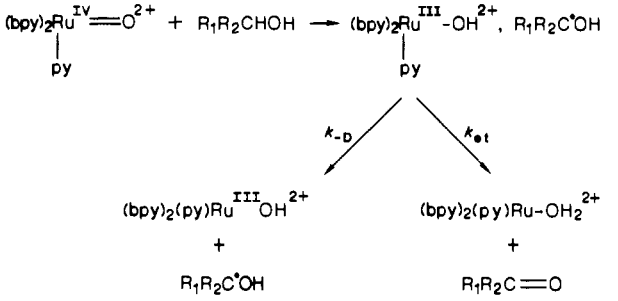

complexes in which the reactants have the appropriate relative orientation(s) for the redox step to occur.

The question remains as to the nature of the redox step. In earlier work based on the oxidation of alcohols by Ce(IV), V(V), Mn(III), and Cr(VI), either direct or kinetic evidence is available to suggest the formation of discrete, inner sphere metal–alcoholate complexes which decompose via homolytic or heterolytic pathways.[23-26] The reactions exhibit a range of kinetic isotope effects ranging from k_H/k_D = 1.9 for the oxidation of cyclohexanol by Ce(IV), to k_H/k_D = 3.6 for the oxidation of cyclohexanol by V(V), to k_H/k_D = 7 for the oxidation of 2-propanol by Cr(VI). The kinetics of the processes are usually described by relatively complex, proton dependent rate laws.

It is conceivable that oxidation by Ru(IV) occurs via coordination sphere expansion through a seven-coordinate intermediate

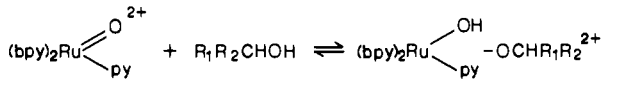

followed by an intramolecular redox step. However, a prior intermediate seems unlikely given the following: (1) There is no evidence for the appearance of an intermediate early in the stopped-flow traces. (2) There is no precedence for coordination sphere expansion at Ru in this coordination environment for these substitution inert complexes. (3) The rate of $H_2{}^{18}O$ exchange with the bound oxo group, which could logically proceed via an intermediate like $[(bpy)_2(py)Ru^{IV}(OH)_2]^{2+}$, appears to be slow. Rather, it appears that, mechanistically, $Ru^{IV}{=}O^{2+}$ should be grouped with the oxo-containing reagents such as permanganate whose reactions are characterized by large, negative $\Delta S^{\ddagger}$ values (e.g., –38 eu for benzhydrol[27]), sizeable k_H/k_D primary kinetic isotope effects (k_H/k_D = 16 for $C_6H_5CH(OH)CF_3$[28]), and simple rate laws.

Net hydride transfer could also occur via initial H atom transfer followed by a second rapid, one-electron step before the initially formed products, Ru^{III}–OH^{2+} and R_1R_2COH, escape from the immediate solvent cage (Scheme II). If this were the case, it follows from the spectral evidence and lack of oxygen dependence of the observed rate constants (O_2 is a known scavenger for the intermediate organic radicals)[10] that $k_{et} > k_{-D}$ in Scheme II. Given reasonable estimates for k_{-D}, if a one-electron mechanism were operative, k_{et} would have to be ≥ 3–4×10^9 s^{-1}.[10]

A number of lines of evidence, however, suggests that the oxidation of hydrocarbons by Ru(IV)=O occurs by two-electron steps involving either hydride transfer[9] or C–H insertion:[30] (1) the oxidation of allylic C–H bonds in aromatic hydrocarbons by $Ru{=}O^{2+}$ must involve two-electron steps on energetic grounds, and hydride transfer has been proposed for the oxidation of formate to CO_2. (2) Rate constants for the oxidation of aromatic

(21) Seok, W. K.; Roecker, L.; Meyer, T. J., manuscript in preparation.
(22) (a) Sutin, N. *Acc. Chem. Res.* **1982**, *15*, 275. (b) Sutin, N. *Prog. Inorg. Chem.* **1983**, *30*, 441.

(23) (a) Ardon, M. *J. Chem. Soc.* **1957**, 1811. (b) Littler, J. S. *J. Chem. Soc.* **1959**, 4135.
(24) Littler, J. S.; Waters, W. A. *J. Chem. Soc.* **1959**, 4046.
(25) Littler, J. S. *J. Chem. Soc.* **1962**, 2190.
(26) (a) Westheimer, F. H.; Nicolaides, N. *J. Am. Chem. Soc.* **1949**, *71*, 25. (b) Kaplan, L. *J. Am. Chem. Soc.* **1955**, *77*, 5469. (c) Rocek, J.; Radkowsky, A. E. *J. Am. Chem. Soc.* **1973**, *95*, 7123.
(27) Stewart, R. *J. Am. Chem. Soc.* **1957**, *79*, 3057.
(28) Stewart, R.; van der Linden, R. *Disc. Faraday Soc.* **1960**, *29*, 211.

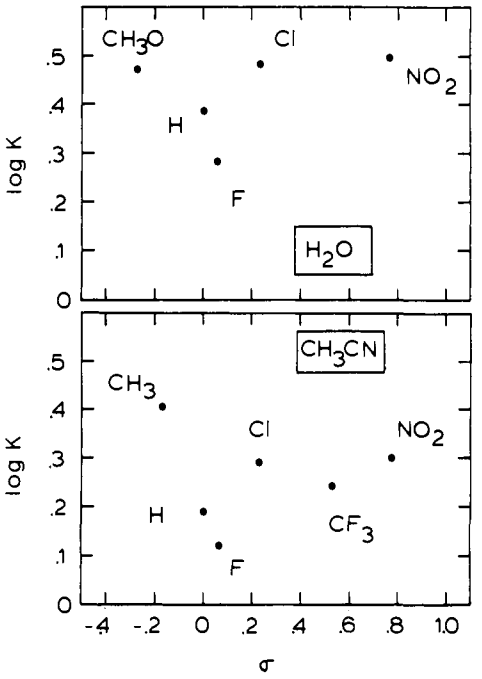

Figure 5. Hammett plots for the oxidation of para substituted benzyl alcohols by $[(bpy)_2(py)Ru(O)]^{2+}$ in acetone/water (upper) and in 0.10 M TEAP/CH_3CN (lower).

hydrocarbons are comparable and even greater than rate constants for alcohol oxidation even though aromatic hydrocarbons are normally far less reactive toward one-electron oxidants.[29] (3) Oxidation of cyclobutanol by $[(trpy)(bpy)Ru(O)]^{2+}$ gives cyclobutanone as the major product,[10] whereas one-electron oxidations characteristically give ring-opened products.[31]

Substituent Effects. The rate of oxidation of alcohols by $[(bpy)_2(py)Ru(O)]^{2+}$ is sensitive to changes in structure of the alcohol. Even without taking into account statistical factors arising from varying numbers of chemically equivalent, oxidizable C–H bonds, the rate constants fall into the following sequence: methyl < primary < secondary < allylic $\lesssim$ benzylic. Although there are insufficient data to draw quantitative conclusions, an important consideration in determining the relative reactivity order is, no doubt, the relative thermodynamic reducing abilities of the series of alcohols.

For the series of benzylic alcohols, k_{obsd} varies essentially randomly as variations in the para substituents are made as shown by the attempt at a Hammett correlation in Figure 5. The absence of a correlation between the electronic properties of the para substituents and the rate was surprising to us given the extensive charge transfer expected for a hydride transfer step.

Although it seems unlikely, some of the sensitivity at the para position could be lost from the fact that $k_{obsd} = k_{redox}K_a'$ and substituent effects in K_a' could mask effects in k_{redox}. A more likely explanation is that local electronic effects induced by the adjacent oxygen atom of the alcohol group overwhelm contributions from the remote para site on the aromatic ring. A related substituent insensitive Hammett plot has been reported for the oxidation of the anions of para substituted fluoro alcohols by permanganate in basic solution; these reactions also have significant k_H/k_D kinetic isotope effects.[28]

Kinetic Isotope Effects. The experimental facts pertaining to the k_H/k_D isotope effects show that they are not amenable to simple interpretation. This is particularly apparent in the oxidation of alcohols by $[(bpy)_2(py)Ru(O)]^{2+}$ where, although a common hydride transfer mechanism may exist, k_H/k_D at 25 °C varies from

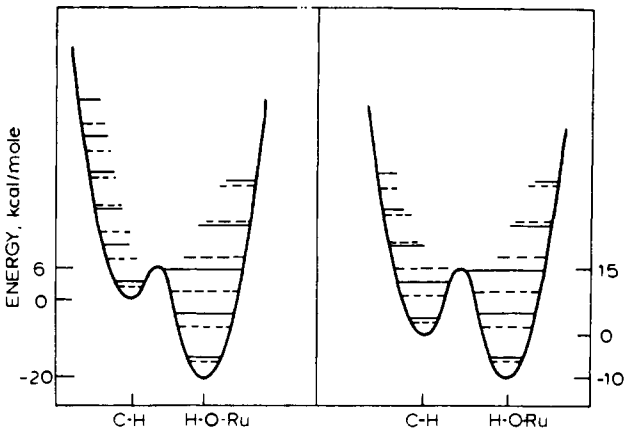

Figure 6. Potential curves for oxidation by $[(bpy)_2(py)RuO)]^{2+}$. In the diagrams are shown the ν(C–H) or ν(O–H) (—) and ν(C–D) or ν(O–D) (– –) vibrational energy levels for the unperturbed vibrations in the reactants $Ru^{IV}{=}O^{2+}{\cdot}H_2RCOH$ and products $Ru^{III}OH^{2+}$, $HRC{=}OH^+$ for benzyl alcohol (left) and methanol (right). The experimental energies of activation are also indicated.

9 for the oxidation of methanol to 50 ± 3 for the oxidation of benzyl alcohol.

Nonetheless, it is significant that for benzyl alcohol the effect is large and *temperature independent* over the temperature range studied, $\Delta H^{\ddagger} = 5.7 \pm 0.2$ kcal/mol compared to $\Delta H^{\ddagger} = 5.6 \pm 0.6$ kcal/mol ($E_a = 6.1 \pm 0.6$ kcal/mol) for $C_6H_5CD_2OH$. The smaller isotope effect for methanol *is* temperature dependent with k_H/k_D ranging from 12 (291 K) to 7 (313 K) and using data taken in the temperature range 291.0–313.2 K, $\Delta H^{\ddagger} = 14 \pm 2$ kcal/mol compared to $\Delta H^{\ddagger} = 17 \pm 2$ kcal/mol for CD_3OH.

Large isotope effects have also been reported for the oxidation of benzhydrol[27] and fluoroalcohols[28] by permanganate. For benzhydrol, $k_H/k_D = 6.6$ (pH 12) while oxidation of the anion of $C_6H_5CH(OH)CF_3$ occurs with $k_H/k_D = 16$. The isotope effect for the anion of the fluoroalcohol is temperature dependent, with $\Delta H^{\ddagger} = 9.1$ kcal/mol and $\Delta S^{\ddagger} = -24$ eu for $C_6H_5CH(O)CF_3^-$ and $\Delta H^{\ddagger} = 11.3$ kcal/mol and $\Delta S^{\ddagger} = -22$ eu for $C_6H_5CD(O)CF_3^-$.

The temperature dependence of k_H/k_D has been treated for simple outersphere electron transfer where electronic coupling between reactants is weak.[32] In treatments of this kind electron transfer occurs as a nonadiabatic transition from the vibrational levels of the initial (reactants) to final (products) potential curves. Transition rates are higher for levels near the intersection region between potential curves because overlap of vibrational wavefunctions between the initial and final states is higher. Maximum: k_H/k_D isotope effects are predicted to occur at low temperatures where transitions are dominated by levels close to $v = 0$ since the lower zero point energy ($^1/_2h\nu$) for the deuterium-substituted case ensures that the vibrational overlap differences between the ν(A–H) and ν(A–D) modes are maximized. When not at the low temperature limit, a larger E_a is expected for the deuterium case because of the importance of thermal population of levels nearer the intersection region where vibrational overlaps are higher.

The situation here is far more complex. There is no orbital basis for strong electronic coupling in either the reactants, $Ru^{IV}{=}O^{2+}$, $H{-}C(OH)R_1R_2$, or products, $Ru^{II}{-}OH^+$, $R_1R_2COH^+$, given the outersphere nature of their interaction. Nonetheless, a *significant* electronic coupling between the $d_\pi(t_{2g}$ in O_h symmetry) acceptor orbitals at Ru(IV) and σ(C–H) in the alcohols *must* occur which is strongly coupled with the ν(C–H) vibrational mode. Most certainly the reaction does not proceed by anything approaching formation of a free hydride ion—$Ru^{IV}{=}O^{2+}$, $H{-}C(OH)R_1R_2 \rightarrow Ru^{IV}{=}O^{2+}$, H^-, $R_1R_2COH^+$—and the time dependent, vibrationally induced electronic coupling between reactants is the key feature to understand about the reactions. Any quantitative assessment of the hydride transfer must take

(29) (a) *Oxidation in Organic Chemistry*; Wiberg, K. B., Ed.; Academic Press: New York, 1965. (b) Benson, D. *Mechanisms of Oxidation by Metal Ions*; Elsevier: New York, 1976.
(30) Dobson, J. C.; Seok, W. K.; Meyer, T. J., work in progress.
(31) Rocek, J.; Radkowsky, A. E. *J. Am. Chem. Soc.* **1973**, *95*, 7123.
(32) (a) Buhks, E.; Bixon, M.; Jortner, J. *J. Phys. Chem.* **1981**, *85*, 3763. (b) Guarr, T.; Buhks, E.; McLendon, G. *J. Am. Chem. Soc.* **1983**, *105*, 3763.

into account in an explicit manner the vibrationally induced electronic coupling.

Given the nature of the hydride pathway, the dominant vibrational contributors to the reaction are clearly normal modes having appreciable ν(C–H) character in the alcohol reductant, ν(Ru=O) in the Ru(IV) oxidant, and ν(H–ORu) and ν(HO–Ru) character in the Ru(II) product. In Figure 6 are shown the following for the hydride transfer step in the oxidation of methanol and benzyl alcohol: (1) Harmonic oscillator potential curves for the ν(C–H) and ν(H–ORu) modes. (2) The various energy quantities appropriate to the hydride transfers including the approximate internal energy changes for the redox steps and the energies of activation near room temperature. (3) The curves connecting the harmonic oscillators are schematic attempts to illustrate a linear combination of the Q(C–H) and Q(H–ORu) coordinates which are important in leading to strong electronic coupling between $Ru^{IV}=O^{2+}$ and H–C(OH)R_1R_2 and their conversion to products. More realistic models are available for hydrogen-atom pathways such as H atom abstraction from CH_3OH or CH_3CN in low-temperature glasses.[33] In such treatments an assumption is made concerning the form of the potential curve, and vibrational overlap or "tunneling" calculations are made for the transition rates.

We have no detailed information concerning the shapes of the potential curves for alcohol oxidation and the temperature range for which we have data is too small to provide a basis for curve fitting. However, some reasonable conclusions can be drawn and predictions made: (1) Given the existence of vibrationally induced electronic coupling, the potential curves in Figure 6 are functions of the appropriate electronic and nuclear coordinates of the reactants and products. The curves will become significantly anharmonic near the crossing, and the quantum spacings are expected to decrease as the top of the barrier is approached. The temperature effects on k_H/k_D near room temperature in the oxidation of CH_3OH suggest that transitions below the top of the barrier play an important role and help explain the magnitude of the greater E_a for CD_3OH. (2) For benzyl alcohol the effective tunneling distance between Q_{eq}(C–H) and Q_{eq}(H–ORu) must be smaller than for methanol, and hydride transfer is dominated by transitions from $v = 0$ in ν(C–H) which gives the maximum k_H/k_D kinetic isotope effect. For methanol the tunneling distance is longer, and advantage is gained by thermal activation to levels higher in the vibrational manifold where vibrational overlap is enhanced. (3) With this interpretation hydride transfer from benzyl alcohol occurs at the *low-temperature limit* in the quantum mechanical sense for the ν(C–H) mode. (4) Over a larger temperature range a considerable curvature is expected in the ln k vs. $1/T$ plots for alcohols like methanol. At lower temperatures a greatly *enhanced* k_H/k_D isotope effect, possibly exceeding 50 is to be expected for methanol as well. At sufficiently high, probably experimentally inaccessible temperatures a decreased k_H/k_D isotope effect is to be expected for benzyl alcohol when thermal populations of higher vibrational levels where the tunneling distance is smaller becomes significant. (5) The large negative entropies of activation, $\Delta S^{\ddagger} \sim -40 + 2$ eu, have their origins in K_a' through the association and selective orientational demands of the reactants, but there is also a significant contribution from the vibrational overlap or tunneling factors. The evidence for this conclusion is direct given the appearance of the k_H/k_D kinetic isotope effect for benzyl alcohol solely in the temperature independent term: $\Delta S^{\ddagger} = -38 \pm 1$ eu for $C_6H_5CH_2OH$ and $\Delta S^{\ddagger} = -46 \pm 2$ eu for $C_6H_5CD_2OH$. In the low-temperature limit, the difference $\Delta(\Delta S^{\ddagger}) = -8$ eu is a direct measure of the difference in tunneling factors between ν(C–H) and ν(C–D). Methanol appears to be a distinctive case with $\Delta S^{\ddagger} = -26 \pm 6$ eu, in part, perhaps arising from a more favorable K_a'. However, vibrational overlap effects must also play a role given the *increase* in $\Delta S^{\ddagger}$ for CD_3OH ($\Delta S^{\ddagger} = -21 \pm 5$) which is consistent with an important contribution to the rate process from thermal population of a level or levels above $v = 0$ for which vibrational overlaps are higher.

Table IV. Comparative Kinetics Data for the Oxidation of Alcohols by Oxo Reagents

oxidant	substrate	$\Delta H^{\ddagger}$ (kcal/mol)	$\Delta S^{\ddagger}$ (eu)	k_H/k_D[a]	ref
$[(trpy)(bpy)Ru(O)]^{2+}$	$CH_3CH(OH)CH_3$	9	−34	5.2	10
$[(bpy)_2(py)Ru(O)]^{2+}$	$C_6H_5CH_2OH$	5.7	−38	50	*b*
MnO_4^-	$C_6H_5CH(OH)C_6H_5$	5.7	−38	6.6	27
MnO_4^-	$C_6H_5CH(OH)CF_3$	9.1	−24	16	28
RuO_4	$CH_3CH(OH)CH_3$			4.6	3

[a] k_H/k_D for the C–H bond involved in the net oxidation. [b] This work. [c] 0.02 M OH^-.

Comparison with Other Systems. In an earlier section note was taken of the fact that for oxidants like Ce(IV), V(V), Mn(III), and Cr(VI), alcohol oxidation occurs by prior coordination of the substrate to the oxidant. However, clear similarities appear to exist between the oxidation kinetics of alcohols by $[(bpy)_2(py)Ru(O)]^{2+}$, RuO_4, and MnO_4^- as shown by the data collected in Table IV. From the data, it appears that oxidations of alcohols by these reagents are characterized by substantial k_H/k_D kinetic isotope effects and similar patterns in activation parameters.

Nonetheless, drawing upon the similarities in the parameters listed to conclude that a common mechanism exists is questionable at best. For example, in the oxidation of H_2O_2 by $[(bpy)_2(py)Ru(O)]^{2+}$, which is known to occur by a $1e^-$, H atom transfer, $\Delta H^{\ddagger} = 6.0 \pm 0.3$ kcal/mol, $\Delta S^{\ddagger} = -37 \pm 3$ eu, and $k_{H_2O}{}^{25°C}/k_{D_2O}{}^{25°C} = 21.6 \pm 1.2$.[19] In addition, oxidations by $[(bpy)_2(py)Ru^{III}(OH)]^{2+}$, which are necessarily one-electron in nature, can have similar parameters. For example, the oxidation of 2-propanol in CH_3CN occurs with $\Delta H^{\ddagger} = 10$ kcal/mol, $\Delta S^{\ddagger} = -38$ eu and $k_H/k_D \geq 8$.[10]

Additional, competitive mechanisms may also intervene. For example, oxidation of $C_6C_5CH(OH)CF_3$ by MnO_4^- gives the ketone,[28] but the $Ru^{IV}=O^{2+}$ complexes appear to attack the aromatic ring, in a pathway for which $k_H/k_D \sim 1$.[34]

Implications for Catalysis. A growing number of transition-metal complexes are known to catalyze the oxidation of alcohols, but in most cases the reaction mechanisms are not well-understood.[2] Our study has provided detailed mechanistic information on a coordinatively stable, well-defined system that is also catalytic. The implications of our results for catalysis include the following: (1) a wide variation (10^3) in the rates of alcohol oxidations by $[(bpy)_2(py)Ru(O)]^{2+}$ is observed ranging from the relatively slow oxidation of aliphatic alcohols (ethanol, $k = 2 \times 10^{-3}$ M^{-1} s^{-1}) to the more rapid oxidation of benzylic alcohols (benzyl alcohol, $k = 2.4$ M^{-1} s^{-1}). (2) Rates respond to driving force. Using $[(trpy)(phen)Ru(O)]^{2+}$ which is a stronger oxidant than $[(bpy)_2(py)Ru(O)]^{2+}$ by 100 mV results in a sixfold rate enhancement. (3) pH can influence the rate. We have reported on the electrocatalytic oxidation of benzyl alcohol at pH 12 by $[(trpy)(phen)Ru(O)]^{2+}$ and find a considerable rate enhancement ($k = 24$ M^{-1} s^{-1}) due to reaction of the deprotonated alcohol.[35] (5) The ruthenium complexes can be used in conjunction with chemical cooxidants. In initial experiments we have observed the quantitative conversion of benzhydrol to benzophenone with catalytic amounts of Ru complex and periodate or hypochlorite as cooxidant.[36] (6) Because of the two-electron character of the reaction, high energy, radical intermediates are avoided which eliminates unwanted side reactions. (7) Because of the operation of the hydride transfer mechanism, the lead in O-atom stays in the coordination sphere of the Ru oxidant. As a consequence, there are no substitutional steps at the metal in the catalytic cycle which allow a substitutionally inert complex like $Ru(IV)=O^{2+}$ to be utilized as a catalyst.

(33) Le Roy, R. J.; Murai, H.; Williams, F. *J. Am. Chem. Soc.* **1980**, *102*, 2325.
(34) Roecker, L., unpublished results.
(35) Kutner, W.; Meyer, T. J.; Murray, R. W. *J. Electroanal. Chem.* **1985**, *195*, 375.
(36) Adrian, S.; Roecker, L., unpublished results.

Acknowledgments are made to the National Science Foundation under Grant No. CHE-8304230 for support of this research.

Registry No. CH_3OH, 67-56-1; H_3CCH_2OH, 64-17-5; $H_3C(CH_2)_2OH$, 71-23-8; $H_3CCH(OH)CH_3$, 67-63-0; $H_2C{=}CHCH_2OH$, 107-18-6; $H_2C{=}CHCH(OH)CH_3$, 627-27-0; $C_6H_5CH_2OH$, 100-51-6; 4-$H_3COC_6H_4CH_2OH$, 105-13-5; 4-$O_2NC_6H_4CH_2OH$, 619-73-8; 4-$FC_6H_4CH_2OH$, 459-56-3; $H_3CC_6H_4CH_2OH$, 589-18-4; $C_6H_5CH(CH_3)OH$, 98-85-1; $(C_6H_5)_2CHOH$, 91-01-0; $[(bpy)_2(py)RuO]^{2+}$, 76582-01-9; D_2, 7782-39-0; cyclohexanol, 108-93-0.

Supplementary Material Available: Table A, values of k_{obsd} for the oxidation of the alcohols in 0.1 M TEAP/CH_3CN by $[(bpy)_2(py)Ru(O)]^{2+}$; Table B, values of k_{obsd} for the oxidation of alcohols in aqueous solution by $[(bpy)_2(py)Ru(O)]^{2+}$ (7 pages). Ordering information is given on any current masthead page.

Carbon Dioxide Chemistry and Electrochemistry of a Binuclear "Cradle" Complex of Ni(0), $Ni_2(\mu\text{-}CNMe)(CNMe)_2(PPh_2CH_2PPh_2)_2$

Dru L. DeLaet, Renato del Rosario, Phillip E. Fanwick,† and Clifford P. Kubiak*

Contribution from the Department of Chemistry, Purdue University, West Lafayette, Indiana 47907. *Received July 16, 1986*

Abstract: The binuclear Ni(0) complex, $Ni_2(\mu\text{-}CNMe)_2(CNMe)(dppm)_2$, **1**, undergoes two one-electron oxidations ($E_{1/2}$ = −0.51 and −0.83 V vs. Ag/AgCl) to form the complex, $Ni_2(\mu\text{-}CNMe)(CNMe)_2(dppm)_2^{2+}$, **2**. The crystal structure of **2** as the PF_6^- salt has been determined. Complex **2** crystallized in the space group $P2_1$ with a = 13.659 (3) Å, b = 14.852 (4) Å, c = 17.970 (3) Å, β = 101.44 (1)°, V = 3573.0 (2) Å^3, and Z = 2. The structure was refined to convergence (R = 0.056, R_w = 0.073) for 4036 unique data over the range $4° \le 2\theta \le 45°$ by using Mo Kα radiation. Complex **2** exhibits an unusual *trans,cis*-diphosphine configuration at the Ni centers and contains a semibridging isocyanide. The electrochemical behavior of **2** in the presence of CO_2 has been examined. Complex **2** reacts with CO_2 by an EC electrochemical mechanism to afford the CO_2 complex $Ni_2(\mu\text{-}CNMeCO_2)(CNMe)_2(dppm)_2$, **3**. Complex **3** also has been prepared by reaction of **1** with CO_2(l). Prolonged reaction of **1** with CO_2(l) leads to complete carbonylation and $Ni_2(\mu\text{-}CO)(CO)_2(dppm)_2$, **4**. The results of labeling experiments using $^{13}CO_2$ and 99% ^{13}C-enriched $Ni_2(\mu\text{-}^{13}CNMe)(^{13}CNMe)_2(dppm)_2$ are interpreted in terms of a reaction pathway involving O-atom transfer from CO_2 to the carbon atom of the bridging isocyanide of **1**.

The activation and reduction of carbon dioxide are areas of intense interest.[1-3] The preparation, structure, and N-alkylation chemistry of the "cradle"-type complex $Ni_2(\mu\text{-}CNMe)(CNMe)_2(dppm)_2$, **1** (dppm = bis(diphenylphosphino)methane) were recently described.[4] We now report the role the nucleophilicity of the μ-methyl isocyanide ligand of complex **1** plays in activating the CO_2 molecule. We also report the 2e$^-$ redox chemistry of **1**. Together, the chemical and electrochemical characteristics of **1** provide an interesting opportunity for electrochemically induced CO_2 activation.

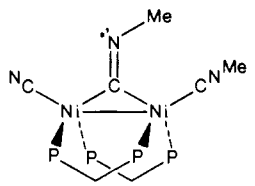

1

Experimental Section

Materials and Physical Measurements. All manipulations were performed in an N_2 atmosphere by using Schlenk techniques or a glovebox. Solvents were reagent grade and were distilled over the appropriate drying agents. $K^{13}CN$ and $^{13}CO_2$ (99 atom %) were purchased from Aldrich Chemical Co. Methyl isocyanide was prepared by literature procedures.[15,16] ^{1}H NMR and ^{31}P NMR spectra were recorded on a Varian XL-200 spectrometer. The ^{31}P chemical shifts are reported relative to 85% H_3PO_4 and ^{1}H chemical shifts to Me_4Si. Infrared spectra were recorded on a Perkin-Elmer 1710 FTIR. Microanalyses were performed by Galbraith Laboratories by using a LECO high-temperature analyzer.

Preparation of $Ni_2(\mu\text{-}CNMe)(CNMe)_2(dppm)_2$ (1). Complex **1** was prepared as recently reported[4] or by reduction of a benzene slurry of $[Ni(CNMe)_4][PF_6]_2$ with Na/Hg in the presence of bis(diphenylphosphino)methane.

Preparation of $[Ni_2(CNMe)_3(dppm)_2]^{2+}$ (2). $[Ni_2(CNMe)_3(dppm)_2][BF_4]_2$ (**2**) was isolated by electrolytic oxidation of **1** at 0.00 V vs. Ag/AgCl. A solution of 0.037 g of **1** in 0.1 M TBAF/THF was placed in the center compartment of a three-compartment cell which was contacted by a glassy carbon working electrode. A Pt gauze counter electrode contacting $[FeCp_2][PF_6]$/electrolyte solution and Ag/AgCl reference electrode were placed in the counter and reference electrode compartments, respectively. The average current density over 6 h was

† Author to whom correspondence pertaining to crystallographic studies should be addressed.

(1) Darensbourg, D. J.; Kudaroski, R. A. *Adv. Organomet. Chem.* **1983**, *22*, 129.
(2) Palmer, D. A.; Van Eldik, R. *Chem. Rev.* **1983**, *83*, 651.
(3) Eisenberg, R.; Hendriksen, D. E. *Adv. Catal.* **1979**, *28*, 79.
(4) DeLaet, D. L.; Fanwick, P. E.; Kubiak, C. P. *Organometallics* **1986**, *5*, 1807.
(5) Chatt, J.; Kubota, M.; Leigh, G. J.; March, F. C.; Mason, R.; Yarrow, D. J. *Chem. Commun.* **1974**, 1033.
(6) Karsch, H. H. *Chem. Berichte* **1977**, *110*, 2213.
(7) Aresta, M.; Nobile, C. F.; Albano, V. G.; Forni, E.; Manassero, M. *J. Chem. Soc. Chem. Commun.* **1975**, 636.
(8) Herskovitz, T.; Guggenberger, L. J. *J. Am. Chem. Soc.* **1976**, *98*, 1615.
(9) Tsuda, T.; Sanada, T.; Saegusa, T. *J. Organomet. Chem.* **1976**, *116*, C10.
(10) Woodcock, C.; Eisenberg, R. *Inorg. Chem.* **1985**, *24*, 1285.
(11) (a) Stanley, G. G.; Osborn, J. A.; Bird, P. H. *Abst. Pap.—Am. Chem. Soc.* **1985**, *190*, INOR-365; (b) Stanley, G. G.; Osborn, J. A.; Bird, P. H., unpublished results.
(12) DeLaet, D. L.; Powell, D. R.; Kubiak, C. P. *Organometallics* **1985**, *4*, 954.
(13) Nicholson, R. S.; Shain, I. *Anal. Chem.* **1964**, *36*, 706; *Anal. Chem.* **1965**, *37*, 178.
(14) Rapi, G.; Sbrana, G.; Gelsomini, N. *J. Chem. Soc. C* **1971**, 3827.
(15) Casanova, J.; Schuster, R. E.; Werner, N. D. *J. Chem. Soc.* **1963**, 4280.
(16) Mottern, J. G.; Fletcher, W. H. *Spectrochimica Acta* **1962**, *18*, 995-1003.
(17) Braterman, P. S. *Structure and Bonding*; Springer-Verlag; Berlin, 1976; Vol. 26, pp 13-16.

0002-7863/87/1509-0754$01.50/0